



ELSEVIER

www.elsevier.nl/locate/ica

Inorganica Chimica Acta 294 (1999) 266–274

**Inorganica
Chimica Acta**

Synthesis of organo(siloxo)platinum and -palladium complexes and preparation of supported nanoclusters by facile ligand reduction[☆]

Atsushi Fukuoka¹, Akihiro Sato, Kin-ya Kodama, Masafumi Hirano,
Sanshiro Komiya^{*}

Department of Applied Chemistry, Tokyo University of Agriculture and Technology, 2-24-16 Nakacho, Koganei, Tokyo 184-8588, Japan

Received 14 January 1999; accepted 19 April 1999

Abstract

A series of organosiloxo complexes of platinum and palladium, $MR(OSiPh_3)(L_2)$ ($M = Pt, Pd$; $R = Me, Et, Ph$; $L_2 = cod, dppe$), has been prepared and characterized. The square planar geometries of $PtPh(OSiPh_3)(cod)$ and $PtEt(OSiPh_3)(cod)$ are confirmed by X-ray structure analysis. In the reactions with hydrogen at 0°C and 1 atm, the siloxo complexes of Pt and Pd are reduced readily to give agglomerates of nanoclusters with complete hydrogenation of the ligands. The reduction activities of the siloxo and alkoxo complexes are higher than those of the corresponding alkyl complex $PtMe_2(cod)$. This high activity in reduction is applied to the preparation of supported Pt or Pd nanoclusters on silica, and the siloxo complexes adsorbed on silica are reacted with hydrogen at mild conditions. The resulting Pt/SiO_2 gives a smaller mean diameter than that prepared from H_2PtCl_6/SiO_2 . © 1999 Elsevier Science S.A. All rights reserved.

Keywords: Siloxo complexes; Platinum complexes; Palladium complexes; Crystal structures; Nanoclusters

1. Introduction

Small metal particles with diameters in the range 1–10 nm (i.e. nanoclusters)² attract current interest since they are expected to display unique physical and chemical properties [1]. One major application of the metal nanoclusters is heterogeneous catalysis, in which supported platinum catalysts are used extensively in practical reactions such as naphtha-reforming and NO_x -removal processes [2]. The conventional preparative method of supported metal catalysts is impregnation and hydrogen reduction; the supports such as silica

and alumina are impregnated with metal salts and they are reduced with hydrogen at high temperature (200–400°C). However, the particle size and distribution are still controlled insufficiently for the monodispersed metal nanoclusters by the conventional methods. On the other hand, organometallic compounds are attractive precursors due to their well-characterized structures and potential high activity in reduction at mild conditions. In the past 20 years, supported organometallic compounds, in particular metal carbonyl clusters, were widely applied to heterogeneous catalytic reactions, and in many cases better catalytic performances were obtained than those by the conventional catalysts from metal salts [3].

One of the new preparative methods of nanoclusters is the reduction of low valent metal complexes under mild conditions, in which metal atoms are extruded from labile organometallics with concomitant removal of ligands [1a]. By using this method, low-valent complexes of Pt [4], Pd [5], Ru [6], and Ir [7] were reduced to give highly dispersed nanoclusters in solutions or on supports. Organoplatinum complexes were also used as precursors in chemical vapor deposition [8].

[☆] Dedicated to Professor D.F. Shriver on the occasion of his 65th birthday.

^{*} Corresponding author. Fax: +81-42-388 7500.

E-mail addresses: fukuoka@design.cat.hokudai.ac.jp (A. Fukuoka), komiya@cc.tuat.ac.jp (S. Komiya)

¹ Also corresponding author: Present address: Catalysis Research Center, Hokkaido University, Sapporo 060-0811, Japan. Fax: +88-11-706 4957.

² According to Lin and Finke [7], we define nanoclusters as particles smaller than 10 nm and colloids as bigger ones.

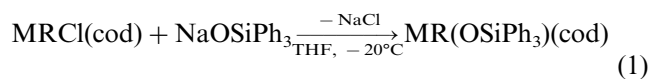
Organosiloxo complexes [9] of transition metals are in a class of alkoxo complexes [10], and they are important not only as precursors in sol-gel chemistry but also as intermediates in several homogeneous catalyses. We are interested in the R–M–O–Si bonds of the siloxo complexes, which may be structure models of active sites on M/SiO₂ catalysts in hydrocarbon conversions. As a part of our study on the reactivity of organoplatinum(II) and related complexes, we found that facile reduction took place for novel organo(siloxo)platinum(II) complexes at 1 atm and 0°C [11]. Here we describe the details of synthesis, characterization, reactivity of the Pt and Pd siloxo complexes, and their application to the preparation of metal nanoclusters on supports.

2. Results and discussion

2.1. Preparation and characterization of Pt and Pd complexes

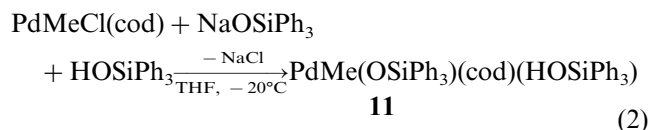
Organoplatinum(II) and -palladium(II) complexes prepared and used in this work are as follows: PtMe(OSiPh₃)(cod) (**1**), PtEt(OSiPh₃)(cod) (**2**), PtPh(OSiPh₃)(cod) (**3**), PtMe(OCPh₃)(cod)(HOCPH₃) (**4**), PtMe(OPh)(cod) (**5**), PtMe(SPh)(cod) (**6**), PtMe(OSiPh₃)(dppe) (**7**), PtMe₂(cod) (**8**), PtMeCl(cod) (**9**), PdMe(OSiPh₃)(cod) (**10**), PdMe(OSiPh₃)(cod)(HOSiPh₃) (**11**) (cod = 1,5-cyclooctadiene, dppe = 1,2-bis(diphenylphosphino)ethane).

Metathetical reactions of PtRCl(cod) (R = Me, Et, Ph) or [PtR(cod)](NO₃) with NaOSiPh₃ in THF under nitrogen gave new siloxo complexes of platinum **1–3** (Eq. (1)). The complexes were purified by recrystallization; for example, colorless blocks of **1** were obtained from Et₂O/hexane. In the preparation of the alkoxo analog **4**, isolation of PtMe(OCPh₃)(cod) was unsuccessful but PtMe(OCPh₃)(cod)(HOCPH₃) (**4**) was obtained in the presence of 1 equiv. of Ph₃COH, in which a Ph₃COH molecule is hydrogen-bonded to the OCPh₃ ligand. The Pd siloxo analogs **10** and hydrogen-bonded **11** were prepared in the same procedures (Eqs. (1) and (2)).



M = Pt; R = Me (**1**), Et (**2**), Ph (**3**)

M = Pd; R = Me (**10**)



The molecular structures of **2** and **3** have been determined by X-ray structure analysis. Crystallographic

Table 1
Crystallographic data for **2** and **3**

	2	3
Formula	C ₂₈ H ₃₂ OSiPt	C ₃₂ H ₃₂ OSiPt
<i>M</i> (g mol ⁻¹)	607.74	655.78
Crystal system	triclinic	triclinic
Space group	<i>P</i> $\bar{1}$ (no. 2)	<i>P</i> $\bar{1}$ (no. 2)
<i>a</i> (Å)	10.522(2)	10.557(4)
<i>b</i> (Å)	13.351(3)	13.702(7)
<i>c</i> (Å)	9.602(2)	10.334(4)
α (°)	104.44(2)	104.94(5)
β (°)	109.96(2)	99.32(3)
γ (°)	84.42(2)	69.79(4)
<i>V</i> (Å ³)	1227.6(5)	1350(1)
<i>Z</i>	2	2
<i>D</i> _{calc} (g cm ⁻³)	1.644	1.612
Radiation (Å)	Mo K α	Mo K α
	0.71069	0.71069
μ (Mo K α) (cm ⁻¹)	57.40	52.86
Temperature	rt	rt
2θ (°)	6 < 2θ < 55	3 < 2θ < 55
Scan type	ω - 2θ	ω - 2θ
No. of collected reflections	5986	6586
No. of unique reflections	5072	4979
<i>R</i> ^a	0.028	0.030
<i>R</i> _w ^b	0.035	0.022
Goodness-of-fit	3.66	1.67

$$^a R = \frac{\sum(|F_o| - |F_c|)/\sum|F_o|}{\sum|F_o|}$$

$$^b R_w = \frac{\sum(w(|F_o| - |F_c|)^2/\sum|F_o|^2)^{1/2}}{\sum|F_o|^2}$$

data are summarized in Table 1, and selected bond distances and angles in Table 2. Fig. 1 shows ORTEP drawings of **2** and **3**, in which both complexes have square planar geometries at Pt. For the ethyl complex **2**, the Pt–O bond distance is 2.003(4) Å, which is in the typical range of Pt–O bonds (1.99–2.07 Å) reported for alkoxo platinum complexes such as Pt(OMe)₂(dppe), PtMe(OMe)(dppe), and PtMe(OCH(CF₃)₂)(PMe₃)₂(HOCH(CF₃)₂) [10c]. The Pt–O–Si angle of 139.5(3)° is larger than the Pt–O–C angles for the above alkoxo platinum complexes (117–123°), but the angle is in the typical range of those for siloxo complexes [12]. The Pt–C(3) and Pt–C(4) bond distances

Table 2
Selected bond distances (Å) and angles (°) for **2** and **3**

2			
Pt–O	2.003(4)	Pt–C(1)	2.052(6)
Pt–C(3)	2.297(6)	Pt–C(4)	2.309(6)
Pt–C(7)	2.099(7)	Pt–C(8)	2.112(7)
Si–O	1.586(4)	C(3)–C(4)	1.37(1)
C(7)–C(8)	1.44(1)	Pt–O–Si	139.5(3)
3			
Pt–O	1.992(3)	Pt–C(1)	2.010(4)
Pt–C(7)	2.096(5)	Pt–C(8)	2.113(4)
Pt–C(11)	2.296(5)	Pt–C(12)	2.285(4)
Si–O	1.589(3)	C(7)–C(8)	1.376(6)
C(11)–C(12)	1.331(6)	Pt–O–Si	144.2(2)

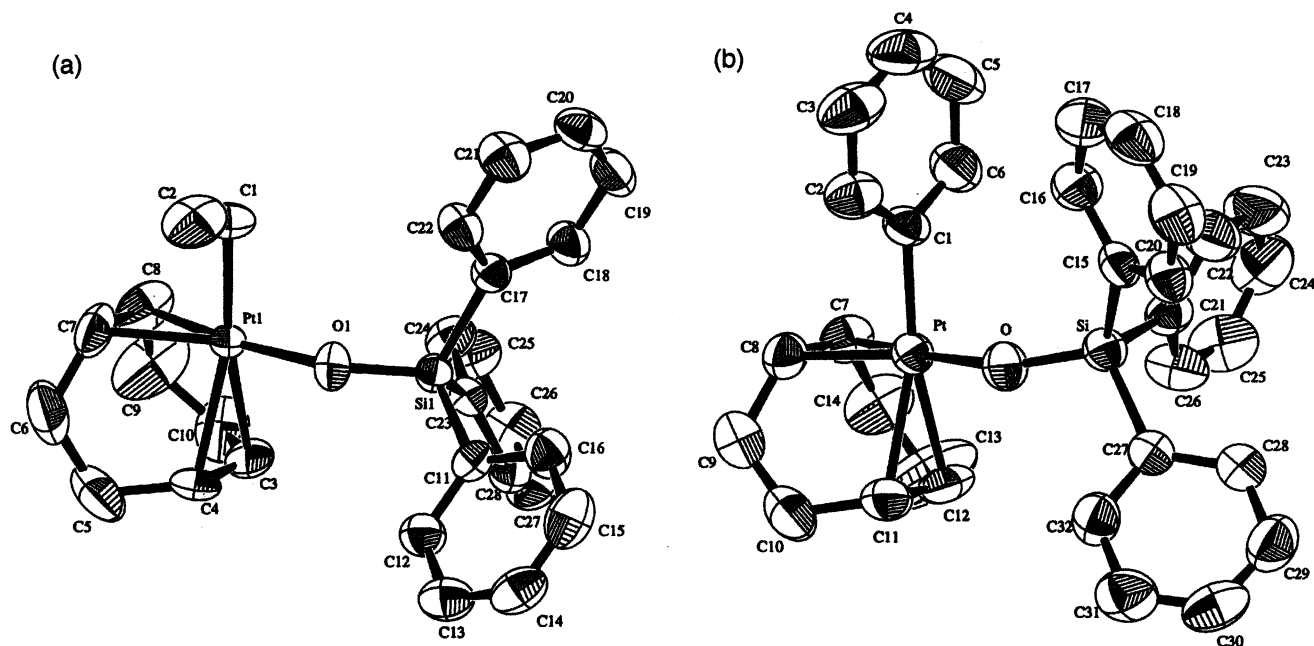


Fig. 1. ORTEP drawings of (a) PtEt(OSiPh₃)(cod) (**2**) and (b) PtPh(OSiPh₃)(cod) (**3**).

distances *trans* to Et are longer than the Pt–C(7) and Pt–C(8) *trans* to OSiPh₃, reflecting stronger *trans* influence of Et than that of OSiPh₃ (see below).

All the new siloxo and alkoxo complexes were characterized by analytical and/or spectroscopic methods. In the ¹H NMR of **1** in C₆D₆, a singlet peak due to the methyl protons appeared at δ 0.95 with ¹⁹⁵Pt satellites. The olefinic protons of COD resonated at δ 3.5 and 5.2 with ¹⁹⁵Pt satellites, whose coupling constants are in accord with the *trans* influence of Me and OSiPh₃ in the square planar geometry; the high field signal with a larger $J_{\text{H-Pt}}$ is due to the olefinic protons *trans* to OSiPh₃ and the low field one with a smaller $J_{\text{H-Pt}}$ to those *trans* to Me. The ¹³C{¹H} NMR of **1** is consistent with the ¹H NMR; the methyl carbon gave a singlet peak at δ 6.9 with ¹⁹⁵Pt satellites, and the olefinic carbons *trans* to OSiPh₃ resonated at δ 74.5 and those *trans* to Me at δ 114.0. The IR spectrum of **1** gave a strong band of $\nu(\text{Si-O})$ at 990 cm⁻¹.

When 3 equiv. of Ph₃SiOH were added to the C₆D₆ solution of **1**, the ¹H NMR signal of *o*-H (δ 8.0) of OSiPh₃ was shifted to high field (δ 7.7), thus approaching δ 7.6 of free Ph₃SiOH with increase in the peak intensity. This shows that the OSiPh₃ ligand exchanges rapidly with free Ph₃SiOH in the solution state. In fact, in the solid state of the Pd analog of **1**, hydrogen-bonded PdMe(OSiPh₃)(cod)(HOSiPh₃) (**11**) was isolated. For the IR spectrum of **11** in KBr, the Si–O frequencies were observed at 916 (s) and 900 (sh) cm⁻¹; the former can be ascribed to the OSiPh₃ ligand and the latter to the hydrogen-bonded HOSiPh₃. Moreover, a broad peak of hydrogen-bonded O–H was seen at 2300–2700 cm⁻¹ as reported for other Pd alkoxo complexes having hydrogen-bonded alcohols

[10f]. On the other hand, in the ¹H NMR of **11** in C₆D₆ the signal of OH was not detected; however, the signal of *o*-H of OSiPh₃ appeared at δ 7.9 slightly higher than δ 8.1 for **10**, approaching δ 7.6 of free Ph₃SiOH. This implies the fast exchange of OSiPh₃ with Ph₃SiOH in the solution state. Similarly, the ¹³C{¹H} NMR of **11** gave signals due to a set of Ph carbons, which also implies the fast exchange of **11** with Ph₃SiOH. Acidolysis of **10** with dry HCl in Et₂O produced CH₄ (95%), Ph₃SiOH (93%), and PdCl₂(cod) (88%). In contrast, the similar reaction of **11** gave CH₄ (96%), Ph₃SiOH (199%), and PdCl₂(cod) (86%), which supports the presence of Ph₃SiOH in **11**.

2.2. Reduction of Pt and Pd complexes

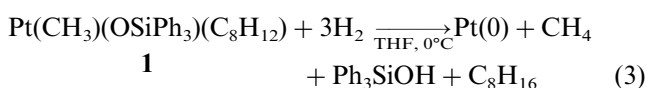
In the investigation of reactivity of the siloxo complexes, the reaction with hydrogen smoothly proceeded at 1 atm and room temperature to form metal colloids. Therefore, we performed the detailed study on the reduction of siloxo and related complexes of platinum and palladium.

Treatment of the THF solution of **1** with H₂ (1 atm) at 0°C precipitated readily a black solid with formation of gas. The GLC, GC-MS, and ¹H NMR analyses revealed that the gas and liquid products were methane, triphenylsilanol, and cyclooctane in quantitative yields. The black solid gave no IR peaks, indicating the absence of organic ligands and products on the solid surface. In the transmission electron microscopy (TEM) observation of the solid, small particles of ca. 3 nm were seen to form agglomerates. These results show that the reaction of **1** with H₂ results in the complete reduction of the metal and ligands (Eq. (3)).

Table 3
Reduction of Pt and Pd complexes MMeX(cod) with hydrogen^a

Sample	Reaction temperature (°C)	Reaction time (h)	Yield (%)		
			CH ₄	HX	C ₈ H ₁₆
PtMe(OSiPh ₃)(cod) (1)	0	1	96	90	99
PtMe(OCPh ₃)(cod)(HOSiPh ₃) (4)	0	1	94	182	89
PtMe(OPh)(cod) (5)	0	1	94	86	90
PtMe(SPh)(cod) (6)	0	1	0	0	0
PtMe(SPh)(cod) (6)	50	1	95	nd	nd
PtMe(OSiPh ₃)(dppe) (7)	0	1	0	0	–
PtMe ₂ (cod) (8)	0	1	0	–	0
PtMe ₂ (cod) (8)	rt	1	186	–	93
PtMeCl(cod) (9)	0	1	0	0	0
PdMe(OSiPh ₃)(cod) (10)	0	1	100	99	92
PdMe(OCPh ₃)(cod)(HOSiPh ₃) (11)	0	1	100	199	101
1/SiO ₂	0	2	96	80	85
5/SiO ₂	0	3	98	76	80
8/SiO ₂	rt	6	186	–	78
10/SiO ₂	0	3	100	78	80

^a Reaction conditions: [complex] = 0.02 M in THF, 0°C, H₂ 1 atm.



Reductions of other Pt and Pd complexes were performed under the same conditions, and yields of ligand hydrogenation are summarized in Table 3. It is notable that the alkoxo (including siloxo and phenoxo) complexes of Pt and Pd gave quantitative yields of methane, cyclooctane, and corresponding alcohols. In contrast, no reaction took place for PtMe(SPh)(cod) (6), PtMe₂(cod) (8), or PtMeCl(cod) (9) at 0°C; thus showing the great effect of X in a series of PtMeX(cod) complexes. The reduction of 6 and 8 proceeded at higher reaction temperatures as reported in the CVD study using 8 [8a]. Substitution of COD to DPPE in 7 inhibited completely the reduction. These results imply that higher reduction activities are obtained for the complexes having more labile ligands.

The reduction activities of the Pt and Pd complexes were compared using the formation rate of methane³. Fig. 2 depicts plots of yields of methane versus time at 0°C and 1 atm in THF. Pd complexes 10 and 11 gave higher rates than Pt complexes, reflecting the general higher reactivity of Pd over Pt complexes. Interestingly, among the PtMeX(cod) complexes the reduction rates of siloxo and alkoxo complexes 1 and 4 were faster than those of the phenoxo complex 5. As described above, complexes 6–9 gave no formation of methane. Accordingly, the order of reduction activity for Pt-

MeX(cod) by changing the ligand X is summarized as follows: OSiPh₃ ≈ OCPh₃ > OPh ≫ SPh, Cl, Me.

For the reduction of 1, the yields of products were plotted against reaction time as shown in Fig. 3, where free COD and cyclooctene were detected at the early stage of the reaction. Therefore, the reaction of 1 with H₂ led to the reduction of methyl and triphenylsiloxy groups with liberation of COD, which was subsequently reduced to cyclooctane via cyclooctene.

Induction periods were observed for the Pt complexes in Figs. 2 and 3, which suggested an autocatalytic process. To clarify the role of the Pt colloids in the reduction of 1, the following experiments were performed (Fig. 4). In the reaction of 1 with H₂ in diglyme ([1] = 0.020 M) at –19°C, the reaction was stopped at ca. 50% conversion after 115 min to form a mixture of 1 and Pt metals. To the resulting mixture was added 1 or 2 equiv. of 1 in diglyme (0.020 M), and in this case

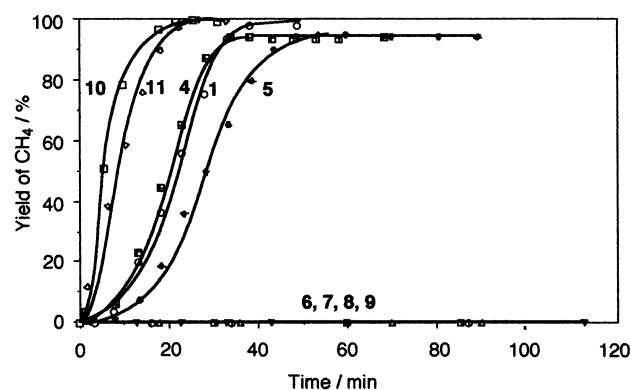


Fig. 2. Plots of yields of CH₄ vs. time in the reduction of Pt and Pd complexes. Conditions: [complex] = 0.02 M in THF, 0°C, H₂ 1 atm.

³ The reduction rate for 1 was independent of the rate of rotation of the magnetic stirring bar, confirming that the reduction was not limited by the diffusion of hydrogen. In this work, 200 rpm was used as a standard rate of rotation.

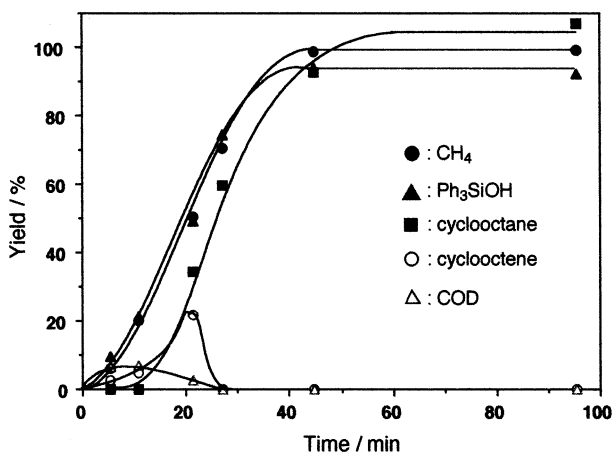


Fig. 3. Plots of product yields in the reduction of **1**. Conditions: $[1] = 0.02$ M in THF, 0°C , H_2 1 atm.

the induction period was not observed. Moreover, the reduction rate was enhanced slightly, however, the determination of the reaction kinetics was unsuccessful. For the CVD on glass or Teflon using $\text{PtMe}_2(\text{cod})$ and related Pt(II) complexes with hydrogen, Puddephatt showed a half-order dependence on the concentration of the precursor complex, and that the reduction process is catalyzed by a preformed platinum metal [8b]. Randall and Whitesides reported that the reduction of $\text{PtMe}_2(\text{cod})$ (**8**) with platinum black is zero-order dependent, which indicates the heterogeneous hydrogenation on the surface of platinum black [13]. In our case, it seems that the surface area of forming Pt particles is insufficient for heterogeneous zero-order reaction, thus providing the complicated reaction profile. Addition of COD and Ph_3SiOH slowed the reduction rate (Fig. 5), implying that the adsorption of Pt complex on the Pt surface is inhibited by forming COD and Ph_3SiOH . From these results and considerations, we propose that the reduction of **1** is catalyzed by the forming Pt metals (Fig. 6).

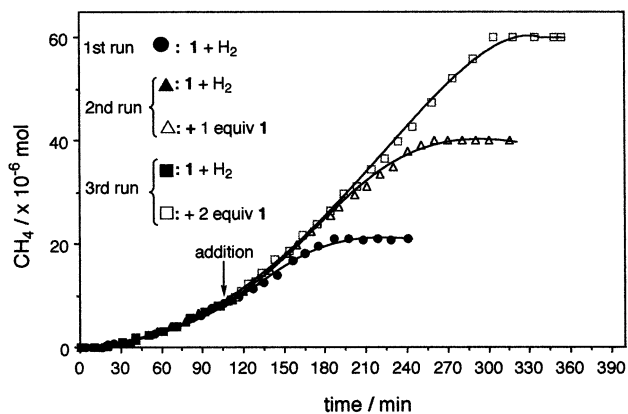


Fig. 4. Effect of addition of Pt colloids in the reduction of **1**. Conditions: $[1] = 0.02$ M in diglyme, -19°C , H_2 1 atm.

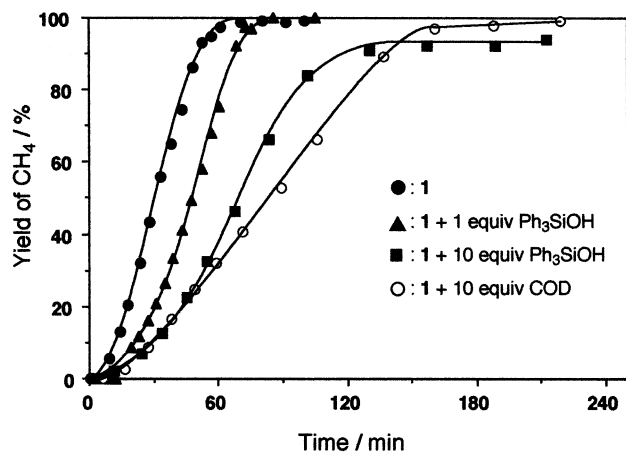


Fig. 5. Effects of addition of Ph_3SiOH or COD in the reduction of **1**. Conditions: $[1] = 0.02$ M in diglyme, 0°C , H_2 1 atm.

The reason for high reduction activity of siloxo and alkoxo complexes is not yet clear. However, the siloxo groups are more labile than SPh, Me, or Cl, as shown by the fast exchange with free silanol. This may result in enhanced adsorption activity of the complexes on the forming Pt metals. Although we performed the test reactions of **1** with several hydrosilanes to study the initial reduction step, observation of Pt hydride or other intermediates was unsuccessful in ^1H NMR even at low temperature.

2.3. Preparation of Pt/SiO₂ and Pd/SiO₂ from organometallics

Since the siloxo and alkoxo complexes of Pt and Pd were highly susceptible to reduction by hydrogen, we applied the high activity in reduction to the preparation of supported metal catalysts. The complexes were adsorbed on silica gel, and the resulting solid was reduced similarly with hydrogen in THF. The color of the solid changed from white to dark gray, and the ligands were hydrogenated completely as shown in Table 3. Ph_3SiOH was also recovered in good yields from the supernatant liquid without adsorption on the silica surface.

The TEM image of Pt/SiO₂ from **1** (designated as Pt(**1**)/SiO₂) is exhibited in Fig. 7 (1 wt% Pt). Black

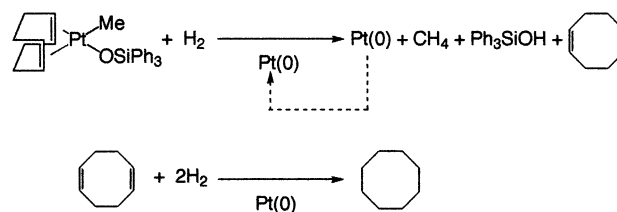


Fig. 6. Possible mechanism for the reduction of **1** with H_2 .

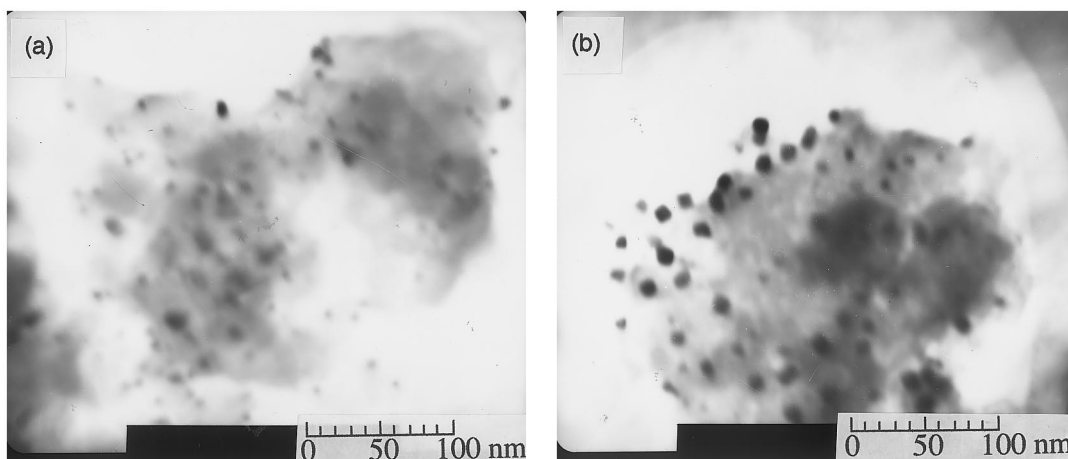


Fig. 7. TEM images of (a) Pt(1)/SiO₂ and (b) Pt(12)/SiO₂.

points seen in the bright field image were identified as crystalline Pt by their selected area diffraction. From the histogram of Pt particle size, the mean diameter of Pt was 8.2 nm (Fig. 8). In contrast, conventional Pt(12)/SiO₂ was prepared from H₂PtCl₆·6H₂O (12) and subsequent O₂ oxidation and H₂ reduction at 400°C. In the TEM of Pt(12)/SiO₂, the mean diameter was 13.2 nm. In addition, the Pt particles of Pt(1)/SiO₂ were distributed more homogeneously than those of Pt(12)/SiO₂. Similarly, Pt/SiO₂ samples were obtained from **5** at 0°C and from **8** at room temperature, and the mean diameters were 5.3 and 9.9 nm, respectively. For Pd(10)/SiO₂ prepared from **10**, the mean diameter of Pd was 7.6 nm. Hence, the benefits of reduction of Pt and Pd compounds are the smaller size and the homogeneous distribution of metal particles on the silica surface. It seems that the mild reaction conditions of 0°C and 1 atm prevent the aggregation of metal particles on the support surface.

The present preparative method of nanoclusters from the siloxo and alkoxo complexes of Pt and Pd has the following advantages. (1) The conditions are mild: 1 atm and below room temperature. (2) Hydrogen as a reductant is separated easily from the reaction solution

without contamination. (3) The reduced ligands are separated easily by filtration. (4) The Pt particles are smaller than those of conventional Pt/SiO₂ from H₂PtCl₆·6H₂O and their distribution is homogeneous.

In summary, we prepared and characterized several siloxo and alkoxo complexes of Pt and Pd. Owing to the highly labile character of the siloxo and alkoxo ligand, reduction of the complexes with hydrogen proceeded under very mild conditions to give metal nanoclusters. Organometallics are useful precursors for nanoclusters, and fine tuning of labile ligands would enable the true control of particle size and distribution.

3. Experimental

3.1. General

All manipulations were performed under a nitrogen or argon atmosphere using standard Schlenk techniques [14,15]. Solvents were dried over and distilled from appropriate drying agents under nitrogen: hexane, toluene, Et₂O, THF, diglyme, and dioxane from Na/

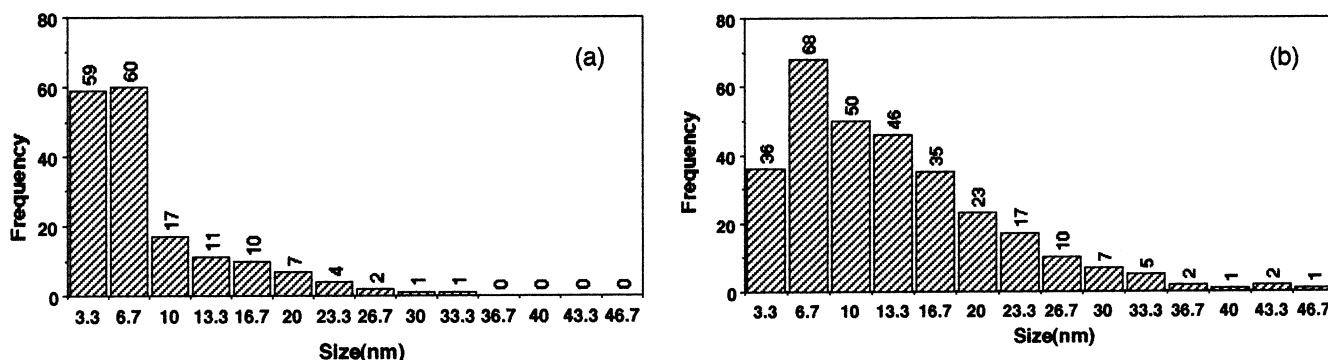


Fig. 8. Histograms of the Pt nanocluster diameters for (a) Pt(1)/SiO₂ and (b) Pt(12)/SiO₂.

benzophenone ketyl. NMR solvents were freeze-pump-thaw degassed and vacuum-transferred from appropriate agents (C_6D_6 from Na; $CDCl_3$ from P_4O_{10}). Pt complexes were prepared according to the literature methods with some modifications: $PtMeCl(cod)$ [16], $PtEtCl(cod)$ [17], $PtPhCl(cod)$ [16], $PtMe(SPh)(cod)$ (**6**) [18], $PtMe_2(cod)$ (**8**) [16], $PdMeCl(cod)$ (**9**) [19], Ph_3SiONa [20]. $KOPh$, $KSPH$, and $NaOCPh_3$ were prepared from potassium (or sodium) with $PhOH$, $PhSH$, or Ph_3COH . NMR spectra were obtained on JEOL FX-200, EX-270, and LA-300 spectrometers. IR spectra were measured on a JASCO FT-IR 5M spectrometer. Elemental analyses were performed with a Perkin-Elmer 2400 series II CHN analyzer. Melting points were measured under nitrogen using a Yazawa capillary melting apparatus and the values were not corrected. Gas chromatography was performed using a Shimadzu GC-8APF with columns of Porapak Q for gases and of PEG 20M for liquids. GC-MS was measured on a Shimadzu GCMS QP2000A using a PEG20M capillary column. Transmission electron microscopy was performed using a Hitachi H-700H microscope.

3.2. Preparation of complexes

A typical procedure for $PtMe(OSiPh_3)(cod)$ (**1**) is given. A Schlenk flask was charged with $PtMeCl(cod)$ (349.2 mg, 0.9871 mmol) and $NaOSiPh_3$ (356.5 mg, 1.195 mmol). THF (15 ml) was added at room temperature and the solution was stirred for 3 h. The mixture was evaporated to dryness and the resulting solid was extracted with toluene. After the filtered solution was again evaporated to dryness, the solid was extracted with Et_2O and addition of hexane gave colorless blocks of **1** (363.1 mg); yield 62%; m.p. 133–134°C (dec.). *Anal.* Calc. for $C_{27}H_{30}OSiPt$: C, 54.62; H, 5.09. Found: C, 54.08; H, 5.37%. IR (KBr, cm^{-1}): 990 (s, $\nu(Si-O)$); 1H NMR (200 MHz, C_6D_6): δ 0.95 (s, $J_{H-Pt} = 75$ Hz, 3H, CH_3), 1.0–2.0 (m, 8H, COD CH_2), 3.5 (br, $J_{H-Pt} = 68$ Hz, 2H, COD =CH *trans* to O), 5.2 (br, $J_{H-Pt} = 27$ Hz, 2H, COD =CH *trans* to C), 7.2–7.3 (m, 9H, $OSiPh_3$ *m*- and *p*-H), 8.0 (m, 6H, $OSiPh_3$ *o*-H). $^{13}C\{^1H\}$ NMR (68 MHz, C_6D_6): δ 6.9 (s, $J_{C-Pt} = 643$ Hz, CH_3), 27.3 (s, $J_{C-Pt} = 22$ Hz, COD CH_2), 31.8 (s, $J_{C-Pt} = 21$ Hz, COD CH_2), 74.5 (s, $J_{C-Pt} = 227$ Hz, COD =CH *trans* to O), 114.0 (s, $J_{C-Pt} = 28$ Hz, COD =CH *trans* to C), 127–129 (m, $OSiPh_3$ *m*- and *p*-C), 135.9 (s, $OSiPh_3$ *o*-C).

$PtEt(OSiPh_3)(cod)$ (**2**) was prepared from $PtEtCl(cod)$ and $NaOSiPh_3$; colorless blocks from Et_2O /hexane; yield 62%; m.p. 102–103°C (dec.). *Anal.* Calc. for $C_{28}H_{32}OSiPt$: C, 55.34; H, 5.31. Found: C, 54.93; H, 5.37%. IR (KBr, cm^{-1}): 1012 (s, $\nu(Si-O)$); 1H NMR (200 MHz, C_6D_6): δ 1.0–2.0 (m, 13H, CH_2CH_3 and COD CH_2), 3.5 (br, $J_{H-Pt} = 73$ Hz, 2H, COD =CH *trans* to O), 5.3 (br, $J_{H-Pt} = 34$ Hz, 2H, COD =CH *trans* to

C), 7.2–7.3 (m, 9H, $OSiPh_3$ *m*- and *p*-H), 8.0 (m, 6H, $OSiPh_3$ *o*-H).

$PtPh(OSiPh_3)(cod)$ (**3**) was prepared from $PtPhCl(cod)$ and $NaOSiPh_3$; colorless blocks from Et_2O /hexane; yield 56%; m.p. 145–146°C (dec.). This complex was identified by spectroscopic methods and X-ray analysis. IR (KBr, cm^{-1}): 990 (s, $\nu(Si-O)$); 1H NMR (200 MHz, C_6D_6): δ 1.0–2.0 (m, 8H, COD CH_2), 3.8 (br, $J_{H-Pt} = 68$ Hz, 2H, COD =CH *trans* to O), 5.4 (br, $J_{H-Pt} = 26$ Hz, 2H, COD =CH *trans* to C), 6.9–7.4 (m, 5H, Pt–Ph), 7.2–7.3 (m, 9H, $OSiPh_3$ *m*- and *p*-H), 7.8 (m, 6H, $OSiPh_3$ *o*-H). $^{13}C\{^1H\}$ NMR (68 MHz, C_6D_6): δ 26.9 (s, $J_{C-Pt} = 21$ Hz, COD CH_2), 31.7 (s, $J_{C-Pt} = 17$ Hz, COD CH_2), 78.1 (s, $J_{C-Pt} = 211$ Hz, COD =CH *trans* to O), 116.0 (br, COD =CH *trans* to C), 124–141 (m, Pt–Ph), 127–130 (m, $OSiPh_3$ *m*- and *p*-C), 135.8 (s, $OSiPh_3$ *o*-C).

A similar reaction of $PtMeCl(cod)$ with $NaOCPh_3$ resulted in the formation of a mixture of $PtMe(OCPh_3)(cod)$ and $PtMe(OCPh_3)(cod)(HOCPh_3)$ (**4**), and isolation of the former was unsuccessful. However, in the presence of 1.1 equiv. of Ph_3COH , **4** was isolated; white needles from THF/hexane; yield 54%; m.p. 65–66°C (dec.). This complex was identified by spectroscopic methods. IR (KBr, cm^{-1}): 1040 (sh, $\nu(C-O)$), 1020 (s, $\nu(C-O)$), 1000 (m, $\nu(C-O)$); 1H NMR (200 MHz, C_6D_6): δ 0.57 (s, $J_{H-Pt} = 78$ Hz, 3H, CH_3), 1.2–2.0 (m, 8H, COD CH_2), 3.5 (br, $J_{H-Pt} = 62$ Hz, 2H, COD =CH *trans* to O), 5.5 (br, $J_{H-Pt} = 27$ Hz, 2H, COD =CH *trans* to C), 7.1–7.2 (m, 18H, Ph *m*- and *p*-H), 7.5 (m, 12H, Ph *o*-H).

$PtMe(OPh)(cod)$ (**5**) was prepared from $PtMeCl(cod)$ and $KOPh$; colorless needles from Et_2O /hexane; yield 56%; m.p. 100–101°C (dec.). *Anal.* Calc. for $C_{15}H_{20}OPt$: C, 43.79; H, 4.90. Found: C, 43.36; H, 4.61%. IR (KBr, cm^{-1}): 980 (s, $\nu(C-O)$); 1H NMR (200 MHz, C_6D_6): δ 0.94 (s, $J_{H-Pt} = 78$ Hz, 3H, CH_3), 1.2–1.9 (m, 8H, COD CH_2), 3.6 (br, $J_{H-Pt} = 68$ Hz, 2H, COD =CH *trans* to O), 5.3 (br, $J_{H-Pt} = 27$ Hz, 2H, COD =CH *trans* to C), 6.9 (t, $J_{H-H} = 7$ Hz, 1H, OPh *p*-H), 7.2 (m, 2H, OPh *o*-H), 7.3 (t, $J_{H-H} = 7$ Hz, 2H, OPh *m*-H).

$PtMe(OSiPh_3)(dppe)$ (**7**) was prepared from $PtMeCl(dppe)$ and $NaOSiPh_3$; yellow powders from Et_2O /hexane; yield 37%; m.p. 193–194°C (dec.). This complex was identified by spectroscopic methods. IR (KBr, cm^{-1}): 996 (s, $\nu(Si-O)$); 1H NMR (200 MHz, C_6D_6): δ 0.98 (dd, $J_{H-P} = 8$ and 4 Hz, 3H, $J_{H-Pt} = 60$ Hz, CH_3), 1.3–1.9 (m, 4H, DPPE CH_2), 6.8–7.1 (m, 12H, DPPE *m*- and *p*-H), 7.2–7.3 (m, 9H, $OSiPh_3$ *m*- and *p*-H), 7.4–7.9 (m, 8H, DPPE *o*-H), 8.0–8.2 (m, 6H, $OSiPh_3$ *o*-H).

$PdMe(OSiPh_3)(cod)$ (**10**) was prepared from $PdMeCl(cod)$ and slight excess $NaOSiPh_3$ in THF at $-20^\circ C$. Colorless blocks were obtained by recrystallization from Et_2O at $-20^\circ C$; yield 62%; m.p. 107°C (dec.).

Anal. Calc. for $C_{27}H_{30}OSiPd$: C, 64.21; H, 5.99. Found: C, 63.89; H, 6.07%. IR (KBr, cm^{-1}): 990 (s, $\nu(Si-O)$); 1H NMR (300 MHz, C_6D_6): δ 1.04 (s, 3H, CH_3), 1.4–1.8 (m, 8H, COD CH_2), 4.0 (br, 2H, COD =CH *trans* to O), 5.6 (br, 2H, COD =CH *trans* to C), 7.2–7.4 (m, 9H, $OSiPh_3$ *m*- and *p*-H), 8.0 (m, 6H, $OSiPh_3$ *o*-H). $^{13}C\{^1H\}$ NMR (75 MHz, C_6D_6): δ 12.7 (s, CH_3), 26.9 (s, COD CH_2), 30.7 (s, COD CH_2), 93.4 (s, COD =CH *trans* to O), 124.2 (s, COD =CH *trans* to C), 127–129 (m, $OSiPh_3$ *m*- and *p*-C), 135.9 (s, $OSiPh_3$ *o*-C), 142.7 (s, $OSiPh_3$ *ipso*-C).

$PdMe(OSiPh_3)(cod)(HOSiPh_3)$ (**11**) was prepared from $PdMeCl(cod)$, $NaOSiPh_3$, and Ph_3SiOH (ratio 1.0:1.3:1.0) in THF at $-20^\circ C$. Colorless blocks were obtained by recrystallization from Et_2O at $-20^\circ C$; yield 55%; m.p. $118^\circ C$ (dec.). *Anal. Calc.* for $C_{45}H_{46}O_2Si_2Pd$: C, 69.17; H, 5.93. Found: C, 69.16; H, 5.97%. IR (KBr, cm^{-1}): 2700–2300 (w, $\nu(O-H)$), 916 (s, $\nu(Si-O)$), 900 (sh, $\nu(Si-O)$); 1H NMR (300 MHz, C_6D_6): δ 0.98 (s, 3H, CH_3), 1.4–1.7 (m, 8H, COD CH_2), 4.0 (br, 2H, COD =CH *trans* to O), 5.6 (br, 2H, COD =CH *trans* to C), 7.2–7.3 (m, 18H, Ph *m*- and *p*-H), 7.9 (m, 12H, Ph *o*-H). $^{13}C\{^1H\}$ NMR (75 MHz, C_6D_6): δ 13.3 (s, CH_3), 26.8 (s, COD CH_2), 30.5 (s, COD CH_2), 94.4 (s, COD =CH *trans* to O), 124.2 (s, COD =CH *trans* to C), 127–130 (m, $OSiPh_3$ *m*- and *p*-C), 135.9 (s, $OSiPh_3$ *o*-C), 139.9 (s, $OSiPh_3$ *ipso*-C).

3.3. Acidolysis of the complexes

The procedure for **1** is given. A sample tube was charged with **1** (21.5 mg, 0.0362 mmol) and degassed. Concentrated H_2SO_4 (1 ml) was added by a hypodermic syringe, and after 4 h the gas phase was analyzed by gas chromatography (Porapak Q): CH_4 97% yield. Acidolysis with HCl was performed in a Schlenk tube, where **1** (20.6 mg, 0.0347 mmol), HCl in Et_2O (1.324 M, 26 μ l), and Et_2O (2 ml) were added. After freeze–pump–thaw degassing, the mixture was stirred at room temperature for 5 h. Gaseous product was analyzed by GLC: CH_4 2%. The mixture was evaporated to dryness, and to the resulting solid was added C_6D_6 . The 1H NMR showed the formation of $PtMeCl(cod)$ (77%) and Ph_3SiOH (80%).

Products and yields in acidolysis with conc. H_2SO_4 : **2**, C_2H_6 (94%); **10**, CH_4 (100%); **11**, CH_4 (93%). With HCl: **10**, CH_4 (95%), Ph_3SiOH (93%), $PdCl_2(cod)$ (88%); **11**, CH_4 (96%), Ph_3SiOH (199%), $PdCl_2(cod)$ (86%).

3.4. X-ray structure analyses of **2** and **3**

A typical procedure for **2** is given. A crystal of suitable size was sealed in a thin-glass capillary under nitrogen. The intensity data were collected at room temperature on a Rigaku AFC-5R diffractometer using

Mo $K\alpha$ radiation ($\lambda = 0.71069 \text{ \AA}$) in the $6 < 2\theta < 55^\circ$ range, and 5986 reflections were collected. Absorption correction was applied to the intensity data. The structure was solved by the heavy-atom methods [21] and refined by a full matrix least-squares techniques using the teXan program [22]. The non-hydrogen atoms were refined anisotropically. Hydrogen atoms were included but not refined. Final R and R_w values are 0.028 and 0.035 for 5072 reflections with $|F_o| > 3\sigma|F_c|$.

3.5. Reduction of Pt and Pd complexes with hydrogen

A typical procedure for **1** is given. A three-way Schlenk flask was charged with **1** (0.020 mmol) and THF (1 ml), and the mixture was freeze–pump–thaw degassed. The flask was placed in a thermostat at $0^\circ C$, and filled with hydrogen (1 atm, ca. 40 molar excess) through a septum rubber using a hypodermic syringe needle. The mixture was stirred at 200 rpm, and the gas phase was periodically analyzed by GLC (Porapak Q) to determine the amount of produced methane. After the reaction, the flask was opened and cyclooctane was analyzed by GLC (PEG 20 M). The mixture was evaporated to dryness, and after adding C_6D_6 the yield of Ph_3SiOH was determined by 1H NMR comparing Ph_3SiOH (*o*-H of Ph) and dioxane as an internal standard. The resulting black solid was washed with Et_2O and was dried under vacuum.

3.6. Preparation of Pt/SiO₂ and Pd/SiO₂

Silica gel (JRC-SIO-4, Catalysis Society of Japan, $374 \text{ m}^2 \text{ g}^{-1}$, 60–100 mesh) was dried under vacuum (10^{-3} Torr) at $200^\circ C$ for 2 h. To a mixture of the silica (571.4 g) and THF (10 ml) was added a THF solution of **1** (17.4 mg) under nitrogen. After stirring for 3 h, all of **1** was adsorbed on the silica, which was confirmed by the 1H NMR of the supernatant liquid. THF (10 ml) was added to the resulting solid, and the mixture was stirred at $0^\circ C$ and 2000 rpm after introduction of hydrogen (1 atm). When the yield of methane reached ca. 100% in the GLC of the gas phase, the reaction was stopped. From the GLC of the supernatant liquid, the yield of cyclooctane was 85%. The liquid was evaporated to dryness, and the yield of Ph_3SiOH was 80% from the 1H NMR of the resulting solid. The solid $Pt(\mathbf{1})/SiO_2$ was washed with Et_2O and dried under vacuum.

Conventional $Pt(\mathbf{12})/SiO_2$ was prepared by the impregnation method. To a mixture of silica (ca. 0.5 g) and water (10 ml) was added a water solution (10 ml) of $H_2PtCl_6 \cdot 6H_2O$ (ca. 13 mg). After stirring for 24 h, the mixture was evaporated to dryness and the resulting solid was dried under vacuum (10^{-3} Torr). The solid was oxidized by O_2 flow at $400^\circ C$ for 2 h, and was cooled to room temperature with Ar flow. Subse-

quently, the solid was reduced by H₂ flow at 400°C for 2 h.

3.7. TEM of Pt/SiO₂ and Pd/SiO₂

The powdered sample was dispersed in butanol and the mixture was mixed by ultrasound. The image was obtained at 200 kV and original magnification was 250 000 ×. Histograms of particle size were obtained from the following sample populations: Pt(1)/SiO₂ 162, Pt(5)/SiO₂ 291, Pt(8)/SiO₂ 240, Pt(12)/SiO₂ 303, Pd(10)/SiO₂ 303.

4. Supplementary material

The bond distances and angles, atomic coordinates, anisotropic displacement parameters, observed and calculated structure factors for the X-ray crystallography of **2** and **3** are available.

Acknowledgements

We thank Professor T. Noma for useful advice on TEM. This work was supported by Tokuyama Science Foundation and by a Grant-in-Aid for Scientific Research from the Ministry of Education, Science, Sports and Culture, Japan.

References

- [1] (a) J.S. Bradley, *Clusters and Colloids*, in: G. Schmid (Ed.), VCH, Weinheim, 1994, p. 459. (b) G. Schmid, *Chem. Rev.* 92 (1992) 1709. (c) G. Schmid, *Applied Homogeneous Catalysis with Organometallic Compounds*, in: B. Cornils, W.A. Herrmann (Eds.), VCH, Weinheim, 1996, p. 636. (d) H. Bönemann, W. Brijoux, *Advanced Catalysts and Nanostructured Materials*, in: W.R. Moser (Ed.), Academic Press, San Diego, 1996, p. 165. (e) M.T. Reetz, W. Helbig, *J. Am. Chem. Soc.* 116 (1994) 7401. (f) Y. Wang, N. Toshima, *J. Phys. Chem. B* 101 (1997) 5301.
- [2] G. Ertl, H. Knözinger, J. Weitkamp (Eds.), *Handbook of Heterogeneous Catalysis*, Wiley-VCH, Weinheim, 1997.
- [3] (a) Y.I. Yermakov, B.N. Kuznetsov, V.A. Zakharov, *Catalysis by Supported Complexes*, Elsevier, Amsterdam, 1981. (b) Y. Iwasawa (Ed.), *Tailored Metal Catalysts*, D. Reidel, Dordrecht, 1986. (c) B.C. Gates, L. Guzzi, H. Knözinger (Eds.), *Metal Clusters in Catalysis*, Elsevier, Amsterdam, 1986. (d) J.M. Bassett, *Industrial Applications of Homogeneous Catalysis*, in: A. Mortreux, F. Petit (Eds.), D. Reidel, Dordrecht, 1988, p. 293. (e) M. Ichikawa, *Adv. Catal.* 38 (1992) 283. (f) A. Fukuoka, M. Ichikawa, J.A. Hriljac, D.F. Shriver, *Inorg. Chem.* 26 (1987) 3643.
- [4] P. Gallezot, D. Richard, G. Bergeret, in: R.T.K. Baker, L.L. Murrel (Eds.), *ACS Symposium Series No. 437*, American Chemical Society, Washington DC, 1990, p. 150.
- [5] J.S. Bradley, E.W. Hill, S. Behal, C. Klein, *Chem. Mater.* 4 (1992) 1234.
- [6] (a) N. Kitajima, A. Kono, W. Ueda, Y. Moro-oka, T. Ikawa, *J. Chem. Soc., Chem. Commun.* (1986) 674. (b) A. Duteil, R. Quéau, B. Chaudret, R. Mazel, C. Roucau, J.S. Bradley, *Chem. Mater.* 5 (1993) 341.
- [7] Y. Lin, R.G. Finke, *J. Am. Chem. Soc.* 116 (1994) 8335.
- [8] (a) N.H. Dryden, R. Kumar, E. Ou, M. Rashidi, S. Roy, P.R. Norton, R.J. Puddephatt, J.D. Scott, *Chem. Mater.* 3 (1991) 677. (b) R.J. Puddephatt, *Polyhedron* 8 (1994) 1233. (c) Z. Xue, H. Thridandam, H.D. Kaesz, R.F. Hicks, *Chem. Mater.* 4 (1992) 162. (d) C.D. Tagge, R.D. Simpson, R.G. Bergman, M.L. Hostetler, G.S. Girolami, R.G. Nuzzo, *J. Am. Chem. Soc.* 118 (1996) 2634.
- [9] (a) H. Schmidbaur, M. Bergfeld, *Inorg. Chem.* 5 (1966) 2069. (b) H.-F. Klein, H.H. Karsch, *Chem. Ber.* 106 (1973) 1433. (c) L. D'Ornelas, A. Choplin, J.M. Basset, L. Hsu, S.G. Shore, *Nouv. J. Chim.* 9 (1985) 155. (d) P. Braunstein, M. Knorr, A. Tiripicchio, M.T. Camellini, *Angew. Chem., Int. Ed. Engl.* 28 (1989) 1361. (e) R. LaPointe, P.T. Wolczanski, *J. Am. Chem. Soc.* 108 (1986) 3535. (f) F.J. Feher, J.F. Walzer, R.L. Blanski, *J. Am. Chem. Soc.* 113 (1991) 3618.
- [10] (a) M.A. Bennett, G.B. Robertson, T. Yoshida, *J. Am. Chem. Soc.* 95 (1973) 3028. (b) T. Yoshida, T. Okano, S. Otsuka, *J. Chem. Soc., Dalton Trans.* (1976) 993. (c) H.E. Bryndza, J.C. Calabrese, M. Marsi, D.C. Roe, W. Tam, J.E. Bercaw, *J. Am. Chem. Soc.* 108 (1986) 4805. (d) K. Osakada, Y.-J. Kim, A. Yamamoto, *J. Organomet. Chem.* 382 (1990) 303. (e) K. Osakada, Y.-J. Kim, M. Tanaka, S. Ishiguro, A. Yamamoto, *Inorg. Chem.* 30 (1991) 197. (f) Y. Kim, K. Osakada, A. Takenaka, A. Yamamoto, *J. Am. Chem. Soc.* 112 (1990) 1096.
- [11] A. Fukuoka, A. Sato, Y. Mizuho, M. Hirano, S. Komiya, *Chem. Lett.* (1994) 1641.
- [12] K. Young, E.D. Simhon, R.H. Holm, *Inorg. Chem.* 24 (1985) 1831.
- [13] T. Randall, G.M. Whitesides, *Acc. Chem. Res.* 25 (1992) 266.
- [14] D.F. Shriver, M.A. Drezdson, *The Manipulation of Air-Sensitive Compounds*, 2nd ed., Wiley, New York, 1986.
- [15] S. Komiya (Ed.), *Synthesis of Organometallic Compounds—A Practical Guide*, Wiley, New York, 1997.
- [16] H.C. Clark, L.E. Manzer, *J. Organomet. Chem.* 59 (1973) 411.
- [17] H.C. Clark, L.E. Manzer, *J. Organomet. Chem.* 33 (1971) 241.
- [18] A. Fukuoka, Y. Minami, N. Nakajima, M. Hirano, S. Komiya, *J. Mol. Catal. A* 107 (1996) 323.
- [19] F.T. Ladipo, G.K. Anderson, *Organometallics* 13 (1994) 303.
- [20] J.F. Hyde, O.K. Johansson, W.H. Dautt, R.F. Fleming, H.B. Laudenslager, M.P. Roche, *J. Am. Chem. Soc.* 75 (1953) 5615.
- [21] SAPI91: H. Fan, *Structure Analysis Programs with Intelligent Control*, Rigaku Corporation, Tokyo, Japan, 1991.
- [22] teXan: *Crystal Structure Analysis Package*, Molecular Structure Corporation, 1985 and 1992.